Journal of Aircraft

VOLUME 3 JULY-AUGUST 1966 NUMBER 4

Inference of Clear Air Turbulence by Means of an Airborne Infrared System

Sol M. Norman* and Norman H. Macoy†
Barnes Engineering Company, Stamford, Conn.

Various researchers have shown that some forms of clear air turbulence are characterized by temperature gradients, of the order of 3° to 5°C. A prototype airborne infrared system has been developed to remotely detect this type of temperature discontinuity at ranges in excess of 10 miles. The detection system is a novel infrared spectrometer consisting of a rocking Fabry-Perot etalon that scans its narrow wavelength pass band from approximately 13.5 to 14.5 μ at the edge of the CO_2 absorption band. Since the infrared transmission is a strong function of wavelength in this spectral region, the instrument sees sequentially shorter atmospheric path lengths during the course of the scan. This permits a temperature discontinuity ahead of the aircraft to be detected by a change in the normal instrument output produced during a scan. The instrument is described in detail, and a comparison is made between it and other types of infrared techniques for this application. Typical output wave shapes for various idealized temperature discontinuities are presented, as well as results from initial field trials.

I. Introduction

THE increasing operational hazards associated with clear air turbulence (CAT) and their possible implications in several air disasters has served to dramatize the urgency of developing a technique that can warn a pilot of the imminence of these hazards. Methods of achieving a CAT warning system have concentrated on airborne systems, because CAT is a microscale phenomenon that cannot be detected by our relatively sparse net of weather stations.

Some of the techniques that are currently being considered include the use of 1) laser systems that operate on the degree of backscatter of energy from the laser beam, 2) sensors to detect the electrostatic field, 3) advanced types of radar, and 4) methods of detecting temperature gradients that are associated with the phenomenon.

Although our knowledge of the mechanism and suitable indicators of CAT is very limited, there exists a variety of data that shows a relationship between sharp horizontal temperature gradients and the occurrence of CAT. Merritt and Wexler[1] have reviewed some of this data and have shown examples (see Fig. 1) of horizontal temperature profiles associated with CAT. Typically, these gradients exhibit a 3° to 5°C temperature change over distances of 3 to 20 miles. In view of this type of temperature relationship, Merritt and Wexler suggested the possibility of a radiometer technique for remotely detecting the presence of CAT.

Although Kadlec[2] has obtained additional data that verify the relationship of temperature gradients with the occurrence of CAT, McLean,[3] in a review of project Jetstream data, has raised doubts regarding the uniqueness of the relationship. An attempt to resolve these questions is beyond the scope of this paper. However, Kadlec is currently engaged in additional flight testing that should be of considerable value in clarifying this question.

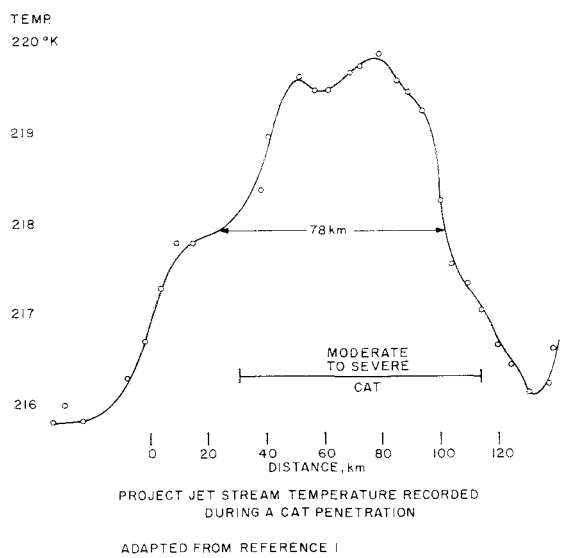

Fig. 1 Typical temperature discontinuity recorded during CAT.

Presented as Preprint 65-459 at the AIAA Second Annual Meeting, San Francisco, Calif., July 26–29, 1965; submitted August 18, 1965; revision received January 10, 1966. The authors gratefully acknowledge the generous and invaluable assistance of R. W. Astheimer during all phases of this program from its conception. We wish to thank also A. F. Turner of Bausch and Lomb. Inc. for his discussions concerning long wavelength low absorption optical coatings, and D. Q. Wark and H. E. Fleming of the U. S. Weather Bureau for discussions concerning the analytical aspects of data reduction.

* Assistant Chief Engineer, Field Research and Systems Department; now Senior Staff Engineer, Sanders Associates, Nashua, N. H.

† Project Engineer, Field Research and Systems Department; now at the Perkin-Elmer Corporation, Norwalk, Conn.

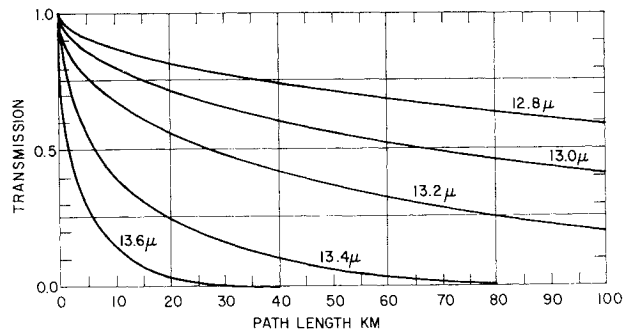

Fig. 2 Transmission of atmosphere at 30,000-ft alt.

The instrument described below has been designed on the premise that there is a useful correlation between horizontal temperature gradients and clear air turbulence. It is based on a novel spectrometer concept that provides advantages over other infrared systems that might be considered for CAT detection. A prototype flight model has been constructed to permit the feasibility of the concept to be verified in flight tests. The use of this type of instrument for the detection of CAT was originated by Astheimer,[4] and was developed on a Barnes Engineering Company sponsored program.

II. Basic Principle of Operation

A. Physical Picture

This section will attempt to provide a brief physical picture of how a spectrometer can be used to measure the temperature gradient of the atmosphere. The spectral transmission of the atmosphere in the infrared is characterized by strong absorption bands. At the center of these bands the atmosphere is essentially opaque, whereas in the region between these bands, the atmosphere is essentially transparent. The transition from an opaque region to its adjoining transparent region is a gradual one. This transition region, or wing of the absorption band, is the key to the measurement of temperature gradients by means of a spectrometer. Consider what happens as the spectral resolution element of a spectrometer is spectrally shifted along the wing of the absorption band; when the spectral resolution element is at the center wavelength of the absorption band, the instrument only will receive radiation from a short path length in front of it. As the spectral resolution element is shifted to either shorter or longer wavelengths, radiation will be received from increasingly greater path lengths until finally, when the spectral resolution element is completely out of the transition region

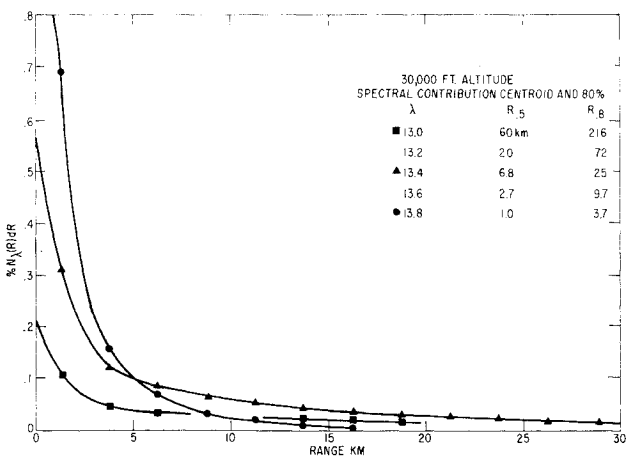

Fig. 3 Distribution of spectral contribution with incremental range.

the instrument will be capable of seeing completely through the atmosphere.

Figure 2 illustrates the variation of transmission with wavelength for the short wavelength edge of the CO_2 absorption band. If each spectral transmission curve of Fig. 2 is redrawn to show how the total energy received at that wavelength is relatively distributed as a function of range, the curves of Fig. 3 result.

The ordinate is labelled $\%\ N_\lambda\ (R)\ dR$ and represents, for various wavelengths, the fractional contribution of energy from a 2.5-km-thick source at a particular range relative to the sum of energy received from the entire path length. These curves can be used as weighting functions that show the relative response of the instrument to each elemental source of emission in front of it for various wavelength settings.

The spectral contribution centroids ($R_{.5}$) indicated on the curves are the ranges at which 50% of the total energy is obtained. Thus, at 13 μ, 50% energy is obtained within the atmospheric path from 0 to 60 km from the instrument, whereas at 13.8 μ, 50% of the energy is obtained within a block of atmosphere from 0 to 1 km. The ranges within which 80% of the energy is received for the various wavelengths are tabulated also under the column labeled $R_{.8}$. (It should be noted that the range scale changes with altitude, i.e., greater distances are measured as altitude increases.)

If the spectrometer is pointed horizontally in an atmosphere having a constant horizontal temperature, it will be found that, throughout the spectral scan of the absorption band, the output of the instrument will correspond to that which would be produced by a blackbody at that temperature. This is because the path lengths are great enough so that total absorption still occurs. The only thing that changes during the scan is the relative weighting of the radiation received from various distances ahead of the instrument. In the assumed constant horizontal temperature atmosphere, this would produce only a blackbody signal variation as a function of the scan. However, if a temperature gradient does exist horizontally, there will be a pronounced change in the signal from the instrument as a function of the spectral scan. This is illustrated in Fig. 4. Here two idealized temperature discontinuities are shown. One discontinuity begins at a distance of 5 km and ends at 100 km; the other begins at 20 km and ends at 100 km. The instrument output for the case of no temperature gradient is also shown; it corresponds to the output that would be obtained if the instrument were measuring a blackbody at atmospheric temperature.

It should be noted that, if a straightforward filter radiometer were pointed into the atmosphere, it would measure the integrated energy for only a single weighting function; this would require a time history of the instrument output to be monitored in order to detect a gradient in the direction of motion of the aircraft.

B. Basic Mathematical Relationships

The preceding discussion has attempted to provide a physical feeling of how a spectral scan can be used to detect the presence of temperature gradients. A more mathematical method of characterizing the relationship between the instrument output and a horizontal temperature gradient was discussed in Astheimer's paper. This will be presented here briefly.

Assume any type of horizontal temperature gradient; this can be approximated by dividing the atmospheric path under consideration into n increments, with each increment characterized by a single temperature.

The radiation signal S_λ received at a given wavelength from the nth increment with respect to a reference temperature will be proportional to the product of its temperature difference with respect to the reference (ΔT_n), the emissivity of the increment $e_{\Delta x}$, and the transmission of the path to the

segment t_{xn}. It is assumed that ΔT is small enough so that the radiation signal will be proportional to the first power of T:

$$S_\lambda = (\Delta T_n)\, e_{\Delta x}\, t_{xn}$$

The total signal will be the summation of the contributions from each increment, which gives a series with as many terms as there are increments. A separate series can be written for each wavelength to form a matrix as shown below:

$$S_\lambda = \sum_{n=1}^{\infty} \underbrace{e_{\Delta x}\, t_{xn}}_{C_n(\lambda)}\, \Delta T_n$$

Therefore,

$$S_{\lambda_1} = C_1(\lambda_1)\,\Delta T_1 + C_2(\lambda_1)\,\Delta T_2 + C_3(\lambda_1)\,\Delta T_3 + \ldots$$

$$S_{\lambda_2} = C_1(\lambda_2)\,\Delta T_1 + C_2(\lambda_2)\,\Delta T_2 + C_3(\lambda_2)\,\Delta T_3 + \ldots$$

$$S_{\lambda_3} = C_1(\lambda_3)\,\Delta T_1 + C_2(\lambda_3)\,\Delta T_2 + C_3(\lambda_3)\,\Delta T_3 + \ldots$$

If we measure the signal in as many wavelengths as we have selected increments, we will have a set of simultaneous equations where the ΔT's are the unknowns. The coefficients $C_n(\lambda)$ are functions of the absorption characteristics of the atmosphere at each particular wavelength which are well known. The ΔT's can then be found by conventional matrix inversion methods. More analytical data processing techniques of the matrices have been developed by the U. S. Weather Bureau for temperature soundings from a satellite borne instrument.[5,12] It is of course essential that the absorption be different in each wavelength or the equations will become degenerate.

C. Interpretation of Instrument Output

The first flight tests will be conducted using recording equipment, thereby permitting detailed postflight analyses of the data to be made. This will establish how well the instrument can measure a temperature gradient. For eventual operational use, it is anticipated that the instrument output can be presented on the screen of an oscilloscope or used to trigger an automatic warning device.

D. Range Capability and Sensitivity Requirements

In the matter of instrument sensitivity, Astheimer showed that at an altitude of 30,000 ft, a 4°C step discontinuity, occurring at a range of 30 km, would produce a signal-to-noise of 9 if the instrument had a NET (noise-equivalent-temperature) of 0.1°C. After planned modifications are completed, the present instrument is expected to achieve this NET by about a factor of 2.

E. Selection of Spectral Region

The preceding discussion has used the CO_2 absorption band in its examples. However, this is not the only absorption band that could be considered. In their paper, Merritt and Wexler considered various atmospheric absorption bands for this temperature measurement. They concluded that the 6.3 μ water absorption band would be most desirable.

The final selection of the optimum absorption band is dependent upon a variety of factors. Some of these depend on the state of the art of infrared detectors as well as on the practicability of cryogenic cooling systems that might make some detector types more desirable. In addition, the possible need for rapid spatial scan may impose a time response requirement that could alter the detector, and hence the absorption band choice. Based on the existing state of the infrared art, our choice of an optimum spectral region is the 12- to 15-μ edge of the CO_2 absorption band. This is based on the following considerations:

1) The CO_2 band is less contaminated by other constituents than are other absorption bands, and it has the most uniform distribution in the atmosphere. In particular, the large variation in moisture content of the atmosphere would be a deterrent to the use of the 6.3-μ water band.

2) The edge of the CO_2 absorption band is wider than the other bands (a more gradual spectral transition from the highly opaque region to the adjacent highly transparent region), thereby making it possible to obtain better range discrimination for the same width of the spectral resolution element.

3) The edge of the CO_2 band is more nearly a smooth function than are the edges of the 4.3- and 6.3-μ absorption bands. McClatchney, however, has pointed out that the stability of the matrix inversion is better if the 4.3-μ band is employed, since dN/dT is greater.[6]

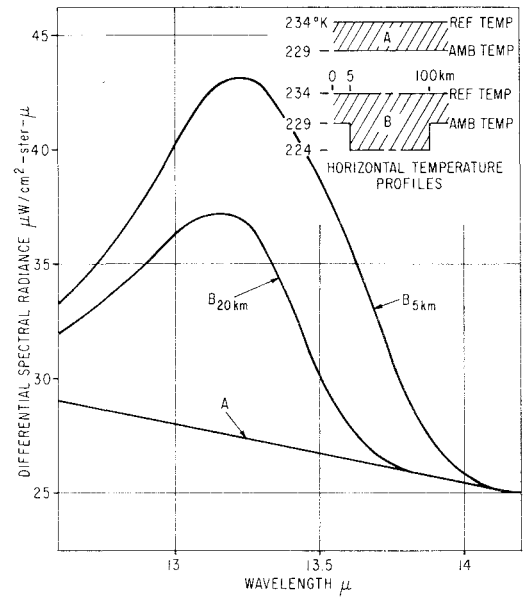

Fig. 4 Radiometric instrument output for idealized horizontal temperature profiles.

F. Similar Concepts

As a final point regarding the basic principle of operation of a spectrometer for the detection of temperature gradients, it should be noted that the approach described here is a variation of a technique that was first suggested by Kaplan[7] for deducing the vertical temperature profile of planetary atmospheres from satellites. This experiment was carried out on the Mariner fly-by of Venus using a two-channel radiometer.[8]

The U. S. Weather Bureau has used three balloon-borne spectrometers for measuring the vertical temperature profile of the earth's atmosphere.[9] These have proved successful, and the Weather Bureau is in the process of acquiring similar spectrometers for use on satellites.

III. Description of Instrument

The instrument that has been developed for remote detection of CAT is essentially a rapid scanning infrared spectrometer. For reasons that are enumerated in a subsequent section, conventional prism or grating spectrometer designs were not selected. Instead, a novel rocking Fabry-Perot interferometer configuration was used. The optical and electronic schematic of the instrument is shown in Fig. 5 and a photograph of it is shown in Fig. 6. It should be noted that the basic instrument configuration is very similar to a conventional radiometer, except that instead of a fixed optical

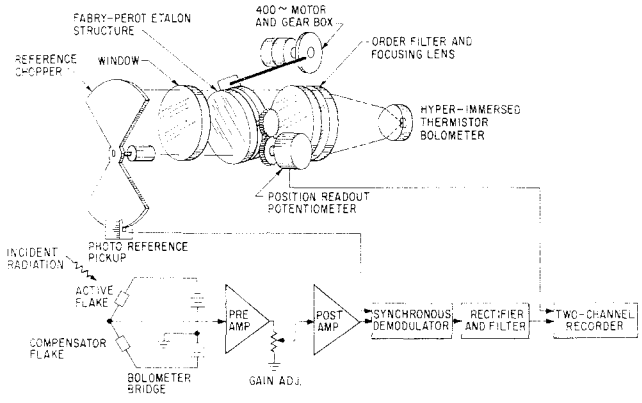

Fig. 5 Fabry-Perot spectrometer optical-electronic schematic.

band pass filter, a rocking Fabry-Perot interferometer and its associated order sorting filter are used. As the interferometer is rocked back and forth relative to the incident energy, its optical band pass shifts as a function of angle, thereby producing the desired spectral scan. The following section describes the principle of operation of the Fabry-Perot interferometer in greater detail.

A. Fabry-Perot Interferometer as a Spectrometer

The Fabry-Perot interferometer consists essentially of two partially reflecting plane mirrors, mounted parallel to each other, called an etalon. The spectral transmission (Fig. 7) of the etalon is determined by two parameters; the optical path μd between the mirrors and the reflectivity r of the surfaces. Constructive interference in transmission occurs at wavelengths fulfilling the following relationship:

$$n\lambda = 2\ \mu d\ \cos\theta$$

where θ = ray angle to the optical centerline, n = order of interference, λ = resonant wavelength, μ = index of refraction of the medium between the two plates, and d = physical separation of the mirrors.

By varying the spacing d, the index μ, or the angle θ, the transmitted wavelength peak is continually shifted, thus providing the desired spectral scan. The present instrument is spectrally scanned by changing the angle θ. Barnes Engineering Company has also fabricated etalons where the spacing d is varied by piezoelectric transducers.

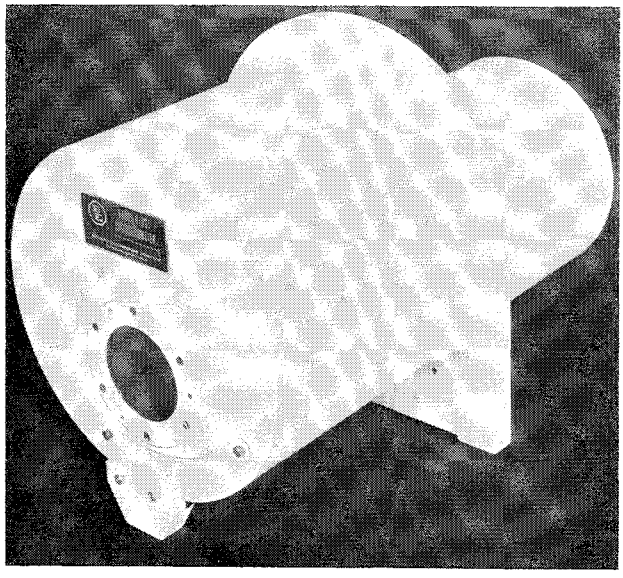

Fig. 6 Infrared scanning Fabry-Perot spectrometer.

Because of the multiple reflections between the two partially reflecting mirrors, the optical fringes (resonances) produced are very sharp (high Q), the sharpness increasing with the reflectivity. This sharpness is one factor in determining the spectral resolution of the etalon. The other factor is the order n that is used. As the order increases, the resolving power $\lambda/\Delta\lambda$ increases; however, this reduces the free spectral range, which is equal to λ/n. The free spectral range must be wide enough to permit the desired spectral scan, and conflicting orders must be eliminated by an order filter.

B. Selection of Optical Design Parameters

The design of the optical section of the instrument is a compromise based on a number of factors. Some of these will be considered briefly.

1. *Spectral resolution*

In determining the spectral resolution, there are two major conflicting requirements. One is the requirement to keep the spectral resolution element as narrow as possible to provide the best range discrimination. The conflicting requirement is to make the spectral resolution element as broad as possible in order to maximize the energy that is received per spectral resolution element. In addition to these factors, other constraints must be considered. One of these is the required free spectral range, since this establishes the highest order at which the etalon can be set. The higher the order, the narrower the resolution.

Another constraint that is associated with the establishment of the order of the etalon is a requirement for a suitable order sorting filter to block wavelengths outside the desired free spectral range. Still another constraint in establishing the resolution is the reflectance of the coatings that are applied to the inner surfaces of the etalon. Achieving high reflectance poses another problem because it reduces the transmission of the etalon in some cases.

The instrument described here has a spectral resolution of 0.35 μ at 14.6 μ. This is wider than is desired, but was chosen as an expediency because available order sorting filters made it necessary to set the etalon for the sixth order instead of for the desired eighth-order spacing. A new order filter is being obtained which will permit the desired order, seven or eight, to be achieved. By using improved coatings on the etalon also, the future spectral resolution expected for the instrument will be approximately 0.2 μ.

2. *Spectral range*

Although the order of the etalon determines the maximum free spectral range, the operating spectral range can be further limited by the amplitude of the angular oscillation employed in tilting the etalon. Therefore, although the present instrument operates in the sixth order and is capable of a free spectral range in excess of 2.4 μ, the spectral region used is selected as 13.1 to 14.6 μ by selecting a suitable amplitude for the angular oscillation. In this case the etalon is oscillated between angular positions of 11° and 28°.

The 13.1 to 14.6 spectral range was selected to facilitate sea level testing at short ranges. For the flight instrument, the spectral scan will be set for approximately 13.7 to 14.7 μ.

3. *Field of view*

Just as was the case in selecting the spectral resolution, conflicting requirements are involved here also. From a sensitivity standpoint it would be desirable to use as large a field as possible. However, this is undesirable in the vertical direction because the instrument would then receive contributions from the vertical temperature gradient. This indi-

cates the desirability of using a rectangular field with the large dimension oriented horizontally. Even then, the horizontal dimension is limited by the largest angle that can be passed through the etalon without degrading the desired spectral resolution. The instrument just described uses a 1.5° × 6.0° field, which appears to be a reasonable compromise for CAT detection.

4. Other optical characteristics

The aperture of the instrument is determined by the size of the etalon plates. The 51-mm-diam plates used in the instrument are very close to the maximum size that is practical to fabricate and adjust to the required tolerances.

Optical materials employed in the instrument are Irtran-4 and Germanium, since both have good transmission qualities in to 13- to 15-μ region. The materials also have favorable indices of refraction, in addition to being reasonably stable when subjected to widely ranging environmental conditions. The etalon plates are Irtran-4 with lead telluride coatings having reflectances of 0.7.

C. Electronic System

The requirements of the electronic system may be summarized as the attainment of linear responsivity, absolute radiometric information, adequate noise free amplification, and adequate temporal resolution. To satisfy the linear responsivity requirement, a bolometer bridge circuit is employed with bias levels set low enough to prevent thermal runaway and stay within limits where Ohm's law is applicable. Absolute radiometric levels are obtained by a reference chopper. The position of the chopper with time is sensed by a photo reference pickup head that generates a synchronous signal that is used for synchronous demodulation.

Noise-free amplification is obtained by two low-noise amplifiers designed for use with thermistor bolometers. A gain potentiometer is also employed to prevent amplifier saturation from occurring. The amplified a.c. signal is synchronously demodulated, rectified, and filtered. The resulting level is then proportional to the radiometric difference between the chopper and the target radiances.

Adequate temporal resolution is necessary in order to permit each spectral resolution element of the etalon to be adequately measured during the scan periods. Temporal resolution was insured by setting the scanning frequency at 1.2 cps, the chopper frequency at 20 cps, and the thermistor time constant at 6 msec.

The instrument just described has the following rms noise equivalents at 300°K: 1) noise equivalent spectral irradiance $NEH_\lambda = 1.0 \times 10^{-6}$ w/cm^2 − sterad-μ; 2) noise equivalent spectral power density $NEPD_\lambda = 1.1 \times 10^{-9}$ (w/cm^2); and 3) noise equivalent spectral temperature $NET_\lambda = 0.094$°C.

These values are not as good as experience and calculations indicate should be achieved by a system of these operating parameters. A factor of 2 improvement in sensitivity is expected when the instrument is further refined and tested.

D. Evolution of the Instrument Configuration

The present instrument embodies two major changes from the configuration that was described earlier in Astheimer's paper. One change is the use of a rocking motion of the entire Fabry-Perot etalon to achieve the desired spectral scan, instead of the arrangement where the two plates of the etalon were mounted on individual piezoceramic cylinders that were driven by suitable voltage variations to change the spacing between the plates. This change was dictated by the loss of time attendant to obtaining redesigned cylinders, and also the time necessary to solve certain engineering problems. Piezoceramic cylinders can be used in this application if the operating mode or environment should indicate this to be desirable.

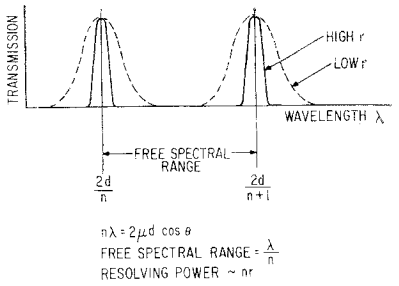

Fig. 7 Characteristics of Fabry-Perot interferometer.

The second major change in the instrument configuration is the use of a reference chopper. This was dicated by two considerations: one was the desirability of obtaining an absolute radiometric signal instead of only the a.c. component in the early flight test evaluations of the instrument; the second consideration came about as a result of using the rocking etalon. In the unchopped system, reflections off the etalon plates permitted energy from the case of the instrument to be seen; this would have necessitated that the system have either no, or at least constant, temperature gradients. In the chopper system, the chopper is the reference, and temperature gradients within the instrument have no effect.

IV. Comparison between the Fabry-Perot Spectrometer and Other Types of Infrared Instruments for the Detection of CAT

A. Radiometer vs Spectrometer

The difference between a radiometer measurement and a spectrometer measurement was described briefly in a preceding section. The radiometer has its optical bandpass set at a given wavelength; therefore, it measures the integrated energy received from a fixed path length ahead of it. The spectrometer's optical bandpass is scanned; therefore, it measures the integrated energy received from sequentially different path lengths ahead of it. With the radiometer approach, a temperature gradient could be detected only by maintaining some record of the output signal until it exhibited a change that was large enough to be caused by a gradient of adequate steepness.

However, with a spectrometer, there is no need to monitor the history of the signal output; each scan progressively compares the near field integrated temperature with the far field integrated temperature, as shown by the weighting functions in Fig. 3. This not only provides a more immediate measurement, but also may make it possible to estimate the steepness of the temperature gradient as a further safeguard against false alarms. Another advantage of a spectrometer over a radiometer is that the spectrometer permits gradients to be detected in directions other than in the line of flight of the aircraft.

B. Dispersive Spectrometers vs Interference Spectrometers

In deciding which type of spectrometer to employ, two basic categories of instruments were considered: 1) dispersive spectrometers that employ gratings or prisms, and 2) interference spectrometers.

For this application, the interferometric approach was deemed more desirable because 1) interferometric spectrometers do not use entrance slits and are therefore capable of accepting much more energy than dispersive spectrometers, thus achieving higher sensitivity; 2) interferometric spectrometers are smaller and lighter in weight, thereby making them more suitable for installation on aircraft; and 3) interferometric spectrometers are simpler and less complicated

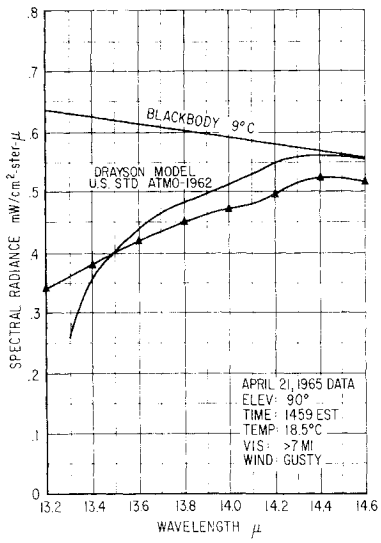

Fig. 8 Spectral radiance vertical temperature lapse rate.

than dispersive spectrometers, and thus the potential cost for production instruments would be less.

C. Fabry-Perot Spectrometer vs Michelson Interferometer Spectrometer

Within the category of interference spectrometers, there are two basic types: the Fabry-Perot and the Michelson. The Fabry-Perot spectrometer was selected for this application in preference to the Michelson because it is less sensitive to vibration, is capable of higher spectral resolution, and requires no complex electronic data conversion technique to obtain a real time output.

V. Results of Initial Field Trials

Prior to seeking support for flight tests, a series of field tests from ground sites were conducted to check the capability of the instrument to detect temperature gradients. The tests were made by pointing the instrument in directions where natural temperature gradients could be expected. The results reported here are from two such tests. Other tests are currently being evaluated. One measurement was vertical and the other was horizontal with the instrument situated near the shore line and pointed out over the ocean. Figures 8 and 9 show the reduced data for the vertical and horizontal measurements, respectively. Both sets of data exhibited anticipated trends. The horizontal data are of special significance since they show a dip that corresponds to the temperature gradient believed to exist in the atmosphere above the shore line. The conditions under which the data were recorded are enumerated in Table 1.

For corollary purposes the data presented in this section are supported by two CO_2 absorption models for the appropriate conditions. The model employed for the vertical temperature lapse rate is based upon the work of Drayson[10] which treats the atmosphere as a finite number of layers with computations of CO_2 transmissions at various spectral intervals in the CO_2 band. Planckian radiometry is then combined with the Drayson work to yield a reference curve shown in Fig. 8. In addition to this reference curve, a blackbody curve for $T = 9°C$ is also presented. This temperature represents the mean temperature for the lowest altitude layer (0 to 1900 m) that was used in Drayson's work. It is clearly seen that, as expected, both curves asymptotically approach the 9°C blackbody curve as the wavelength increases. Vagaries at the shorter wavelengths are caused by the coarseness of the Drayson model.

The model employed for the horizontal temperature profile is based upon the work of Elsasser and of Howard.[11] This model assumes that the CO_2 band consists of equally spaced, equal intensity absorption lines. Planckian radiometry is then combined with a temperature structure defined by

$$T = 15°C \text{ for } 0 \leqslant x \leqslant 2 \text{ km}$$

$$T = 10°C \text{ for } 2 \leqslant x \leqslant \infty$$

to yield the reference curve labelled Elsasser's model in Fig. 9. In addition to this reference curve, a blackbody curve for $T = 15°C$ is also presented. This temperature represents the ambient temperature at the instrument. It is clearly seen that the trend for both curves is to asymptotically approach the 15°C blackbody curve slope as the wavelength increases, just as would be anticipated. The shape and absolute magnitude of the curve which represent data only approximate the Elsasser model curve. Good correspondence between the preceding curves cannot be expected for several reasons; some of the more important reasons are the temperature structure assumed, the inadequacy of the Elsasser model in representing CO_2 absorption, and the spectral radiometric contributions from the relative humidity. Considering the assumptions made, good to excellent correlation has been demonstrated.

VI. Flight Application of the Instrument

A. Aircraft Integration

Opportunities to install the instrument on an aircraft and to perform flight tests are currently being investigated. Because the type of aircraft that may be used is not yet established, it is not possible to describe the detailed integration problems which must be resolved. However, there are certain basic integration problems that must be considered in any aircraft installation and that can be presented briefly here.

1. Varying angle of attack

If angle of attack variations of the aircraft are large during normal level flight, it may be necessary to provide a means to keep the instrument pointed at a constant attitude. This might be necessary in order to avoid sensing the vertical temperature gradient. Two approaches have been considered to accomplish this. One is to mount the instrument on a

Table 1 Conditions for initial field trials

Factors	Conditions
Vertical temperature lapse rate	
Target	Airspace over Barnes Engineering Co., Stamford, Conn.
Date	April 21, 1965
Elev.	90°
Time	1459 EST
Temp.	18.5° C on ground
Vision	>7 miles
Wind	S. easterly, gusty
Instrument alt.	~70 ft above msl
Horizontal temperature profile	
Target	Airspace over Stamford, and Stamford, Conn. harbor
Date	April 21, 1965
Elev.	3°
Time	1405 EST
Temp.	15° C
Vision	Approx. 3 miles light haze
Wind	S. easterly, gusty
Instrument alt.	70 ft above msl
Water temp.	10°C
Distance from shore	2.4 km

rudimentary 1-axis stable platform. The other approach is to use a mirror in the optical system that positions the field of view in response to pitch signals from auto-pilot gyros. It should be noted that, for the initial flight tests, this problem might be surmounted by using data from only those spectral scans that occur when the aircraft is in its normal attitude. If attitude changes occur slowly during the flight i.e., angle of attack changes caused by fuel consumption, the repositioning of the field of view could be accomplished by a manual control.

2. *Achieving an ambient chopper temperature*

It is desirable to have the chopper reference temperature as close as possible to ambient air temperature in order to achieve maximum system sensitivity. The reason for this becomes clear if we consider Fig. 4. Curve A shows the portion of the total signal which is produced by a temperature difference between the chopper reference and the ambient air of 5°C. We are interested only in measuring the increment between curves B and A. Measuring this increment becomes more difficult as A becomes larger. Thus, to avoid this classic problem of attempting to measure a small signal that is superimposed on a large one, we must maintain our chopper reference temperature as close to ambient as possible. Methods for achieving this will depend on the exact aircraft installation, but, in any case, careful thermal design will be required.

3. *Effect of window heating*

Because the window of the instrument is not completely free from absorption, it can provide some radiation signal as its temperature rises above the static ambient as a result of aerodynamic heating. The significance of this contribution is presently undergoing evaluation and a method for optical compensation is being pursued. Electronic compensation is more involved.

B. Flight Testing

The flight tests of the instrument should be conducted in conjunction with other temperature probes, as well as with a suitable means for measuring the magnitude of the turbulence. In this way, there will be a convenient check on how accurately the instrument senses temperature gradients and on how well these gradients are correlated with clear air turbulence.

Other aspects of the anticipated flight test program should include evaluation of the instrument under a variety of meterological conditions, and in various geographical locations. As part of the flight test program it is anticipated that sufficient data will be obtained, so that the instrument parameters such as spectral range, spectral resolution, and scan rate can be optimized.

C. Other Modes of Operation

It should be noted that the instrument can be utilized in other modes of operation that might be of value in the detection and avoidance of CAT. One of these is to incorporate a scanning mirror or perhaps dual optical heads into the system in order to permit regions of turbulence not directly ahead of the aircraft to be observed. Another possible use of the instrument follows from Kadlec's[2] observation that many of his false alarms occurred during penetration of the tropopause. This false alarm rate would be reduced by pointing the field of view of the instrument vertically, thereby permitting the proximity of the tropopause to be established, thus providing advance warning of passage through the tropopause.

Another matter that merits consideration is the possibility of employing the instrument in conjunction with other sensors

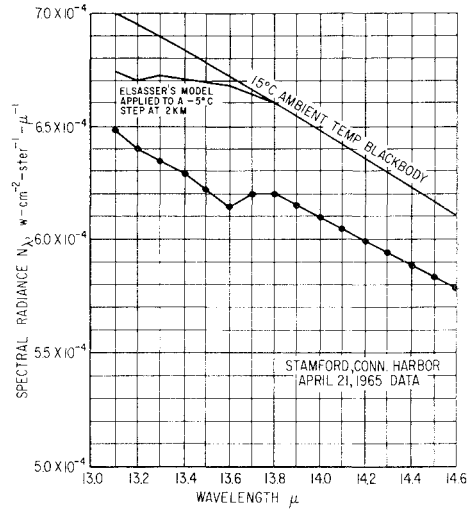

Fig. 9 Spectral radiance horizontal temperature profile.

in order to maximize the detection of CAT. An example of such a sensor would be a radiometer with a narrow bandpass filter at 9.6 μ to detect the presence of ozone. Sensing the presence of zone may prove to be of value, since it is believed that turbulent regions pull down ozone from the stratosphere.

VII. Summary

The following points have been presented:

1) The instrument concept is based on the premise that there is a useful correlation between sharp horizontal temperature gradients and the occurrence of CAT.

2) The principle of operation of the instrument is to detect horizontal temperature gradients by spectrally scanning an edge of the CO_2 atmospheric absorption band.

3) An airborne instrument has been developed to perform this measurement using a novel rocking Fabry-Perot etalon as the means for performing the spectral scan.

4) The Fabry-Perot spectrometer configuration is superior to radiometers as well as to other types of spectrometers for airborne detection of CAT.

5) Initial field trials of the instrument from ground sites indicate that it is capable of detecting temperature gradients in the atmosphere. The tests also indicate the possibility of using the instrument in other meterological applications.

6) Close engineering support will be required in the integration of the instrument with the aircraft in order to obviate possible sources of performance degradation.

7) It is expected that the flight test program will permit the feasibility of the concept to be verified, and will also permit the instrument parameters to be optimized.

References

[1] Merritt, E. A. and Wexler, R., "Radiometric detection of clear air turbulence," Fifth Conference on Applied Meteorology of the American Meteorological Society (March 1964).

[2] Kadlec, P. W., "A study of flight conditions associated with jet stream cirrus, atmospheric temperature change and wind shear turbulence," Eastern Air Lines Inc. Final Report, Contract Cwb-10674 (June 1964).

[3] McLean, G. S., "An investigation into the use of temperature gradients as an in-flight warning of impending clear-air turbulence," Aerospace Instrumentation Lab., Air Force Cambridge Research Labs., Project 6020, Task 602004 (November 1964).

[4] Astheimer, R. W., "An infrared technique for the remote detection of clear air turbulence," *Proceedings of the Third Symposium on Remote Sensing of Environments* (University of Michigan Press, Ann Arbor, Mich., October 1964), pp. 105–123.

[5] Wark, D. Q. and Fleming, H. E., "Indirect measurements of

atmospheric temperature profiles from satellites, I. Introduction," Monthly Weather Rev. (to be published).

[6] McClatchey, R. A., "The use of the 4.3 micron CO_2 band to sound the temperature of a planetary atmosphere," International Symposium on Electromagnetic Sensing of the Earth from Satellites (November 1965).

[7] Kaplan, L. D., "Inference of atmospheric structure from remote radiation measurements." J. Opt. Soc. Am. **49**, 1004–1007 (1959).

[8] Schwarz, F. and Ziolkowski, A., "Two channel infrared radiometer for Mariner II," Infrared Phys. **4**, 113 (1964).

[9] Hilleary, D. T., Wark, D. Q., and James, D. G., "An experimental determination of the atmospheric temperature profile by indirect means" Nature **205**, 489–491 (1965).

[10] Drayson, S. R., "Atmospheric slant path transmission in the 15μ CO_2 band," NASA TR 05863, Contract NASA-54 (03), Office of Research Administration, Univ. of Michigan (November 1964).

[11] Howard, J. N., et al., "Infrared transmission of synthetic atmospheres. IV. Application of theoretical band models," J. Opt. Soc. Am. **46**, 334 (1956).

[12] Fleming, H. E. and Wark, D. Q., "A numerical method for determining the relative spectral response of the vidicons in a nimbus satellite system," Appl. Optics **4**, 337 (1965).

JULY-AUG. 1966 J. AIRCRAFT VOL. 3, NO. 4

Evolution of the Honeywell First-Generation Adaptive Autopilot and Its Applications to F-94, F-101, X-15, and X-20 Vehicles

B. Boskovich* and R. E. Kaufmann†
Honeywell Inc., Minneapolis, Minn.

A review of the considerations that influenced the basic analytical configuration of the Honeywell adaptive autopilot is presented. The control concept uses a wide bandwidth approach with the control gain varied in accordance with information derived within the control system. Desirable performance characteristics have been obtained from the inherent ability of a high-gain feedback control system to accommodate extreme variations in aerodynamic parameters. The gain-changing technique in its early form made use of a bi-stable element. Refinements to the gain-changing technique resulted from practical considerations, such as the influence of pilot inputs, effects of gust disturbances, and the unique performance requirements of various vehicles. The functional requirements, system description, and achieved performance are presented for the F-94, F-101, X-15, and X-20 applications.

Introduction

ALTHOUGH the concept of self-adaptive control systems is not new, most of the serious development effort to design such systems has been expended in the past 10 years. The growing complexity of aircraft control systems, the development of more advanced aircraft, and the advent of winged aerospace vehicles such as the X-15 and X-20 provide the stimulus to spur the effort on. A significant portion of this work was sponsored by the U. S. Air Force Flight Dynamics Control Laboratory of the Research and Technology Division (formerly WADC). At least eight different conceptual schemes have been studied at length by various agencies and investigators. These include systems based upon high-gain, model-following techniques, model reference with error-minimizing schemes, and perturbation response for signal input evaluation. Many of these systems have been developed to the point of proving feasibility in flight tests.

Honeywell has pursued development of the high-gain, model-following concept to a greater extent than any of the other approaches. This basic concept has been developed and tested in a number of vehicles. These include the F-94C, F-101A, X-15, and extensive X-20 hardware simulator studies.‡ This paper describes the functional features, system mechanization, and performance achieved in each case.

Presented at the AIAA/ION Guidance & Control Conference, Minneapolis, Minn., August 16–18, 1965 (no preprint number; published in bound volume of preprints of the meeting); submitted August 15, 1965; revision received January 14, 1966.

* Project Engineer, Aeronautical Division. Member AIAA.

† Principal Development Engineer, Aeronautical Division.

‡ Application has also been made to the control of highly elastic boosters, including design and fabrication of a flight-worthy adaptive controller for test in a Scout vehicle.[1]

Basic Concepts

The Honeywell adaptive autopilot inner loop fundamentally consists of a tight feedback system controlling a selected aircraft variable. This controlled variable is usually selected to facilitate the use of control-stick steering when the autopilot is used as a damper and to facilitate the use of outer loops such as attitude and altitude hold. For this discussion, pitch rate will be considered as the controlled variable, as shown in Fig. 1a.

Comparison of the system in Fig. 1a with conventional pitch rate systems shows few basic differences. There is an important distinction, however, in the response specification. The response of the inner-loop output $\dot{\theta}$ to the input $\dot{\theta}_m$ should be at least three times faster than the desired system response to pilot input commands. Fast response of the inner loop is achieved by using series lead compensation along with high forward-loop gains. Uniformity of the response to input commands is achieved by using an input-shaping model.

Command Response

The desired response to pilot commands for the Honeywell adaptive system is established by a model that shapes all commands to the inner loop. The form of the model and its characteristics are selected on the basis of pilot preference and outer-loop response criteria.

After the model is selected the response requirement for the inner loop may be established. It has been determined experimentally that if the bandwidth of the inner loop exceeds the model bandwidth by a factor of three or more, the over-all response of $\dot{\theta}/\dot{\theta}_c$ essentially will be that of the model. It is evident that once this requirement is achieved, closure of an outer loop such as attitude hold becomes quite convenient. The outer-loop controlled variable need only be related to the